Cyclotron Emission Asymmetry from Kirchhoff's Law in a Mode-Conversion Layer

D. G. Swanson and Suwon Cho
Department of Physics, Auburn University, Auburn, Alabama 36849
(Received 3 February 1989)

Cyclotron radiation of both fast (Alvén) and slow (Bernstein) waves from a mode-conversion layer is considered to find relations between cyclotron absorption and emission in an inhomogeneous plasma. The relative emission ratios among various modes are calculated and asymmetries of emission are discussed. From relations between emission and absorption, a form of Kirchhoff's law for a mode-conversion layer is proved from general thermodynamic arguments and from the mode-conversion tunneling equation.

PACS numbers: 52.25.Sw, 42.20.Cc, 52.35.Hr

While absorption in cyclotron harmonic layers, where both tunneling and linear mode conversion occur, has been studied for many years,[1] the effects of mode conversion on the corresponding emission problem has not been previously analyzed. A comprehensive treatment of the emission from an ion cyclotron harmonic layer which includes the strong dispersive and tunneling effects has appeared recently, but the effects of mode conversion have been omitted.[2] Since we will show that in many cases the energy emitted on the mode-converted branch (a Bernstein mode) exceeds substantially that emitted on the more conventional transverse-Alvén-wave branches, the mode-conversion effects are not perturbative, but rather demand a full-wave analysis of the absorbing-emitting layer. It is the purpose of this paper to establish the fundamental relationship between emission and absorption, embodied in a form of Kirchhoff's law for a mode-conversion layer, without getting into the details of the emission model. This will be done by considering a general thermodynamic or kinetic theory analysis which uses reciprocity relations for a mode-conversion layer, and by considering the specific form of the wave equation which describes the mode-conversion layer.

In order to understand the basic physics of a mode-conversion layer, Fig. 1 illustrates the fundamental character of the dispersion relation in the vicinity of such a layer (without absorption for clarity). The plot shows the dependence of $k_\perp^2$, the wave number perpendicular to the static magnetic field, and z represents a dimensionless distance from the resonance layer in the direction of increasing magnetic field. To be noted is that for large positive z, there are *two* propagating branches, one with $k_\perp \approx$ const, describing a fast Alfvén wave, and another with $k_\perp^2 \propto z$, describing a (slow) Bernstein mode. These two are degenerate at the turning point where linear mode conversion occurs. For large negative z, only the fast wave propagates, and the region between the two turning points is a region of complex $k_\perp$ representing tunneling. Because there are two *kinds* of waves which are coupled linearly, we describe this by a fourth-order wave equation, which in its simplest form may be written in dimensionless form as

$$\psi^{\mathrm{iv}}+\lambda^2 z\psi''+(\lambda^2 z+\gamma)\psi=h(z)\,, \tag{1}$$

where ψ is proportional to the transverse electric field amplitude, γ is proportional to the distance between turning points in Fig. 1 ($\gamma=-1$ corresponds to zero width), λ^2 is the slope of the slow-wave branch, and $h(z)=0$ without any emission or absorption. While this equation was obtained by expanding a dispersion relation,[3] a similar equation has been derived directly from the Vlasov equations whose solutions have the same properties (transmission, reflection, and conversion coefficients) as Eq. (1).[4,5] Since our proofs depend only on the form of the solutions, which are the same, we will restrict our analysis to this simpler equation.

Because this is a fourth-order equation, there are four solutions, only three of which are of interest since one grows exponentially on the left. We define ψ_1 to be the solution which represents a fast wave incident from the right in Fig. 1, ψ_2 represents a fast wave incident from the left, and ψ_3 represents an incident Bernstein wave (from the right). The nature of the coupled solutions is

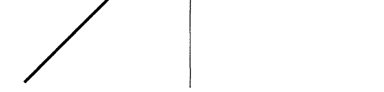

FIG. 1. Sketch of dispersion relation $k_\perp^2(z)$ for $\omega \sim 2\omega_{ci}$. Propagating branches are labeled by the solution, ψ_k, whose incident wave is on the branch shown, and the emitted energy, E_k, radiates along the corresponding branch.

characterized by their asymptotic forms, given in Table I, where $f_\pm \propto e^{\pm iz}$, $s_\pm \propto \exp[\pm(2i/3)\lambda z^{3/2}]$, and $\sigma_\pm$ are growing/decaying exponentials. These asymptotic forms come from the saddle-point integrals from the Laplace solution of Eq. (1) with $h(z)=0$, whence also come the constants of proportionality.[1,6] $f_\pm$ represent fast waves propagating to the right and left, respectively, in Fig. 1, while $s_\pm$ represents slow (Bernstein) waves propagating to the left and right (these are backward waves), respectively. The amplitude transmission (T_j), reflection (R_j), and conversion (C_j) coefficients describe the coupling between these various waves as given in Table I, where the labeling indicates the incident wave branch (except for ψ_4, which grows exponentially). With no absorption, these are[1] $-C_3^-=T_1=T_2=e^{-\eta}$, $D_1=R_1=0$, $C_1=R_2=-\epsilon$, $R_3=e^{-2\eta}$, $-D_2=C_2=e^{-\eta}\epsilon$, and $D_3=C_3^+=-1$, with $\eta=\pi(1+\gamma)/2\lambda^2$, and $\epsilon=1-e^{-2\eta}$.

For a Maxwellian distribution, reciprocity relations have been found numerically[1] and analytically[7] which indicate that the energy fraction transferred from branch i to branch j is the same as from branch j to i. This means that $T_1=T_2=e^{-\eta}\equiv T$, $|C_1|^2/\epsilon=\epsilon|C_3^+|^2\equiv C^+$, and $|C_2|^2/\epsilon=|C_3^-|^2\epsilon\equiv C^-$. The first result shows the fast-wave to fast-wave transmission symmetry. The second result indicates that the fast-to-slow-wave conversion efficiency from branch 1 to 3 is the same as the slow-to-fast-wave conversion efficiency from branch 3 to 1, and the third result is the same result between branches 2 and 3. It is also found that $R_1=0$ whether absorption is included or not[1] [but not for arbitrary $h(z)$, so we allow a general case in Table I]. The appearance of ϵ in these expressions reflects our choice of constant for $f_\pm$. This introduction establishes the basic framework of mode conversion in the presence of absorption.

Thermodynamic result.—For this proof, we assume that there is a perfect absorber on the left and right of Fig. 1, and let $A_1=1-T^2-|R_1|^2-C^+$, $A_2=1-T^2-|R_2|^2-C^-$, and $A_3=1-|R_3|^2-C^+-C^-$ represent the fraction of incident energy absorbed on each of the three branches. We also take E_1, E_2, and E_3 to be the corresponding emitted energy along each of the branches from a single source. Then, if we define I_1, I_2, and I_3 to be the radiated energy from the walls along each of the branches, the outgoing energy along each branch is given by the left-hand sides of

$$E_1+T^2I_2+|R_1|^2I_1+C^+I_3=I_1, \tag{2}$$

$$E_2+T^2I_1+|R_2|^2I_2+C^-I_3=I_2, \tag{3}$$

$$E_3+C^+I_1+C^-I_2+|R_3|^2I_3=I_3, \tag{4}$$

which we equate to the incoming energy on each branch. The equality in Eq. (3) is required because the total energy incident on that wall must balance the total emitted energy from that wall. Although the two other solutions are incident from the same wall, an infinitesimal amount of k_y (vertical wave number) will resolve the two modes spatially, so that they must balance independently. Finally, the law of equipartition of energy demands that a blackbody must radiate the same amount of energy along each independent mode, so $I_1=I_2=I_3=I$. This leads immediately to our result,

$$\frac{E_1}{A_1}=\frac{E_2}{A_2}=\frac{E_3}{A_3}=I, \tag{5}$$

and I depends only on the temperature of the wall. Since this relates emission to absorption mode by mode, we call this the appropriate Kirchhoff's law for a mode-conversion layer. It should be noted that no reference to the form or distribution of either the source or sink has been used for this result. It should also be noted that thermal equilibrium is demanded only of the *wall*, so that any source or sink which yields the reciprocity relations must lead to this result, even if the plasma itself is not in a true equilibrium.

Differential equation result.—In this section, we demonstrate that Eq. (1) leads to the same law as was proved from general arguments. To do this, we use the Green's function for the left-hand side of Eq. (1),[8] which is constructed from the solutions of the mode-conversion–tunneling equation and its adjoint equation which are

$$f^{\mathrm{iv}}+\lambda^2zf''+(\lambda^2z+\gamma)f=0,$$

$$F^{\mathrm{iv}}+\lambda^2zF''+2\lambda^2F'+(\lambda^2z+\gamma)F=0.$$

The adjoint solutions F_k have exactly the same asymptotic relations as f_k except that $F_\pm\sim(2\eta/\pi z)f_\pm$ and $S_\pm\sim-\lambda^2zs_\pm$, both of which are like the ψ_k of Table I except that they both use the homogeneous coefficients.

The sink term for absorption effects for the second-ion-cyclotron-harmonic case is

$$h(z)=-\lambda^2\kappa[\zeta+1/Z(\zeta)](\psi''+\psi),$$

where Z is the plasma dispersion function, $\zeta=(z_a-z)/\kappa$, z_a is the location where the fixed frequency ω is resonant at the harmonic, so that $\omega=2\omega_{ci}(z_a)$, and κ is the normalized parallel wave number. The solution of Eq. (1) is given as $\psi_k(z)=\int_{-\infty}^{+\infty}G_k(z,y)h(y)dy$, where $G_k(z,y)$ is the Green's function for solution ψ_k,[8] given

TABLE I. Asymptotic behavior of solutions of Eq. (1).

$-\infty\leftarrow z$	ψ	$z\rightarrow+\infty$
$T_1f_-+D_1\sigma_-$	$e^{-\eta}\psi_1$	$f_-+R_1f_++C_1s_-$
$f_++R_2f_-+D_2\sigma_-$	$-\psi_2$	$T_2f_++C_2s_-$
$C_3^-f_-+D_3\sigma_-$	$-e^{-\eta}\psi_3$	$s_++R_3s_-+C_3^+f_+$
$\sigma_++C_4^-f_-+D_4\sigma_-$	$-e^{-\eta}\psi_4$	$T_4s_-+C_4^+f_+$

by

$$2\pi i\lambda^2\epsilon G_k(z,y)=\mu_k F_k(y)f_k(z)+\begin{cases}F_1(y)f_2(z)+\epsilon F_0(y)f_4(z) & \text{for } y<z,\\ F_2(y)f_1(z)+\epsilon F_4(y)f_0(z) & \text{for } z<y,\end{cases} \tag{6}$$

where μ_k is a normalizing constant which is chosen such that $\psi_k \to f_k$ as $h(z)\to 0$, and $f_0 \equiv f_3 - f_1$, $F_0 \equiv F_3 - F_1$.

In general, use of the Green's function leads to an integral equation, but for small κ, where the absorption profile is highly localized, $h(z)$ may be approximated by a δ function so that Eq. (1) reduces to

$$\psi^{\text{iv}}+\lambda^2 z\psi''+(\lambda^2 z+\gamma)\psi=2\pi i\epsilon\lambda^2\alpha(\psi''+\psi)\delta(z-z_a)\,,$$

where the constant multiplier α is an arbitrary sink amplitude. Exact solutions are given by

$$\psi_k=f_k+\alpha(\psi_{ka}+\psi''_{ka})\times\begin{cases}F_{1a}f_2(z)+\epsilon F_{0a}f_4(z), & z>z_a,\\ F_{2a}f_1(z)+\epsilon F_{4a}f_0(z), & z<z_a,\end{cases} \tag{7}$$

with $F_{ja}\equiv F_j(z_a)$. Differentiating Eq. (7) twice and adding it to itself, we find

$$\psi_{ka}+\psi''_{ka}=F_{ka}/[1-\alpha(F_{1a}F_{2a}+\epsilon F_{0a}F_{4a})]$$

as well as

$$\psi_k=f_k+\begin{cases}H_{k1}f_2(z)+\epsilon H_{k0}f_4(z) & \text{for } z>z_a,\\ H_{k2}f_1(z)+\epsilon H_{k4}f_0(z) & \text{for } z<z_a,\end{cases} \tag{8}$$

where

$$H_{kj}=\alpha F_{ka}F_{ja}/[1-\alpha(F_{1a}F_{2a}+\epsilon F_{0a}F_{4a})]\,.$$

Strictly speaking, this represents a solution for a sink only at the resonant point, but with the δ function representation, we can consider z_a to be a variable with a different amplitude at each location [so $\alpha=\alpha(z_a)$ in general], so a distributed sink could be represented by a superposition of these solutions.

From these exact solutions, explicit expressions may be obtained for the T_k, R_k (here $R_1\neq 0$ point by point, but the superposition leads to $R_1=0$), and C_k, and the absorbed fractions may then be deduced from the expressions in the introduction, resulting in

$$A_1=e^{-2\eta}|F_1|^2\chi,\quad A_2=|F_2|^2\chi\,,$$
$$A_3=\epsilon e^{-2\eta}|F_3|^2\chi\,, \tag{9}$$

where

$$\chi=2\beta_r-|\beta|^2(e^{-2\eta}|F_1|^2+|F_2|^2+\epsilon e^{-2\eta}|F_3|^2)$$

and

$$\beta=\beta_r+i\beta_i=[1-\alpha(F_{1a}F_{2a}+\epsilon F_{0a}F_{4a})]^{-1}\,.$$

In deriving Eq. (9), we have used $F_1^*=-F_2+\epsilon F_3$, $F_2^*=-e^{-2\eta}F_1-\epsilon F_2-\epsilon e^{-2\eta}F_3$, and $F_3^*=F_1-F_2-e^{-2\eta}F_3$ which can be obtained simply by comparing asymptotic relations in Table I, using the homogeneous $[h(z)=0]$ values of the coupling coefficients.[1]

Generally speaking, any point sink must have a corresponding point source, since any absorber is also an emitter. We may also represent an arbitrary distributed source by a distribution of point sources with appropriate amplitudes, so we will consider an arbitrary point source. For a point source $h(z)=\alpha_e\delta(z-z_e)$, with α_e an arbitrary source amplitude, the emission solution can be obtained by the same method as for the absorption problem except that incoming waves are not permitted. The modified Green's function [setting $\mu_k=0$ in Eq. (6)] leads to

$$\psi_e=\alpha_e\times\begin{cases}F_2(z_e)f_2(z)+\epsilon F_0(z_e)f_4(z), & z>z_e,\\ F_1(z_e)f_1(z)+\epsilon F_4(z_e)f_0(z), & z<z_e.\end{cases} \tag{10}$$

This exact solution leads to the asymptotic result

$$\psi_e\to\alpha_e\times\begin{cases}-F_1(z_e)e^{-\eta}f_+(z)+\epsilon F_3(z_e)e^{-\eta}s_-(z), & z\to\infty,\\ F_2(z_e)f_-(z)+\epsilon F_4(z_e)e^{\eta}\sigma_-(z), & z\to-\infty.\end{cases}$$

This in turn leads to the ratios of emitted energy along the various branches

$$\frac{E_1}{E_2}=e^{-2\eta}\left|\frac{F_1(z_e)}{F_2(z_e)}\right|^2,\quad \frac{E_3}{E_2}=e^{-2\eta}\epsilon\left|\frac{F_3(z_e)}{F_2(z_e)}\right|^2, \tag{11}$$

where E_1 and E_2 are the emitted energy along the fast-wave branches on the high-field side ($z>0$) and the low-field side, respectively, and E_3 is the energy along the slow-wave branch on the high-field side and it is multiplied by the relative energy flux ratio $1/\epsilon$ of the slow wave to the fast wave.[1]

Comparing Eq. (9) with Eq. (11), we discover the relations

$$\frac{A_1}{A_2}=\frac{E_1}{E_2},\quad \frac{A_3}{A_2}=\frac{E_3}{E_2}\,, \tag{12}$$

which are identities as long as $z_e=z_a$ regardless of the value of α or α_e. This leads again to Kirchhoff's law for a mode-conversion layer, but this time the result is a point by point result and follows from the properties of the governing differential equation.

E_1/E_2 and E_3/E_2 are plotted in Figs. 2 and 3 which show strong asymmetries of emission of radiation between branches. Each figure shows the dependence of the asymmetry on the tunneling parameter η, and gives the results for the δ function source at resonance as well

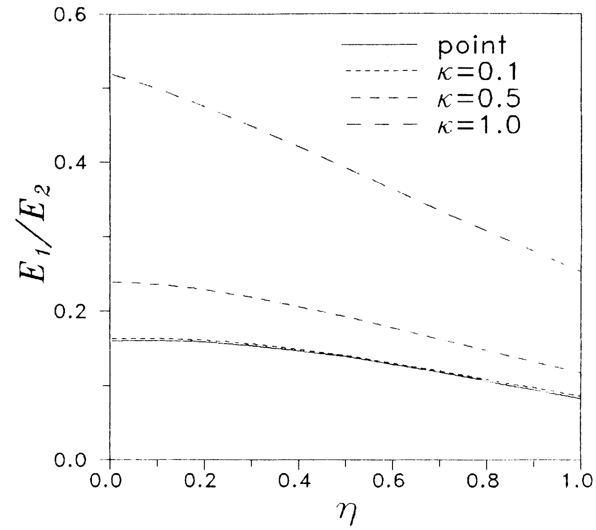

FIG. 2. E_1/E_2 vs η. Solid line relates to the point source at the resonance $z_0 = -\gamma/\lambda^2$ and dashed lines to the distributed source $h(z)$ centered at $z_0 = -\gamma/\lambda^2$.

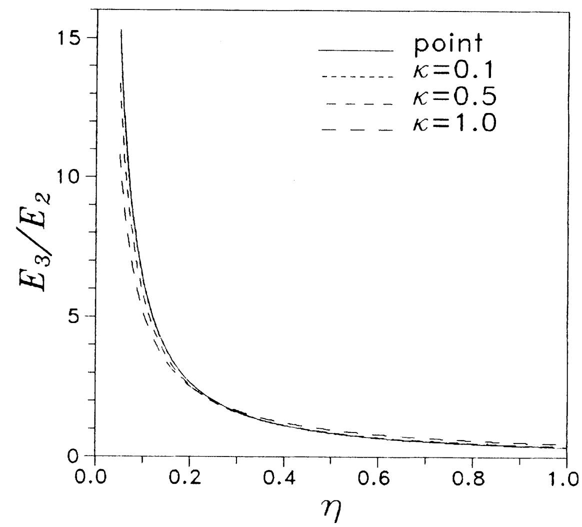

FIG. 3. E_3/E_2 vs η, otherwise same as in Fig. 2.

as the absorption asymmetry dependences for various distributed absorption widths characterized by the normalized parallel wave number, κ. Since Eq. (5) is valid for distributed sources and sinks, then asymmetry results from distributed absorption models give the emission asymmetry for correspondingly distributed sources. The slow wave radiates most of the energy when the tunneling layer is thin (transmitted energy is greater than 50%), and more of the radiation is carried out by the fast wave on the low-field side of the magnetic field than by the fast wave on the high-field side regardless of the tunneling thickness.

While these calculations are explicit for the harmonic $\omega = 2\omega_{ci}$, the same physics applies at higher ion harmonics and at electron cyclotron harmonics. Equation (5) is the generic form for Kirchhoff's law in all cases, indicating that emission is always asymmetric from an inhomogeneous mode-conversion layer. This implies that the absolute magnitude of the radiation from an electron cyclotron resonance layer is always different from that obtained by the simpler models commonly employed which do not include the asymmetry.[9]

It is possible that in actual experiments, the observed asymmetry will be less than that shown, since one never sees only cyclotron emission. A Bernstein wave will invariably be radiated from thermal sources remote from the cyclotron layer and as an incident slow wave, it will be partially converted into the fast wave. The branching ratios for the incident slow wave tend to symmetrize the fast-wave cyclotron emission, but never fully balance the emission unless the remote source is hotter than the resonance layer. If the Bernstein-wave absorption occurs in a lower-temperature region, then the incoming slow wave may have little effect. If the temperature were completely uniform, then the asymmetry would be significantly reduced, but not eliminated.

Since electron cyclotron emission is routinely used as a plasma temperature diagnostic, and ion cyclotron harmonic emission has been proposed as an α particle diagnostic in fusion devices, it would be valuable to have careful measurements of the asymmetry before using the emission intensity as deduced from simpler models as a diagnostic.

This work has been supported by the U.S. Department of Energy under Contract No. DE-FG05-85-ER-53206D.

[1]D. G. Swanson, Phys. Fluids **28**, 2645 (1985). This is a review giving some of the history and an extended bibliography.

[2]D. B. Batchelor, E. F. Jaeger, and P. L. Colestock, Phys. Fluids B **1**, 1174 (1989).

[3]D. G. Swanson, Nucl. Fusion **20**, 949 (1980).

[4]D. G. Swanson, Phys. Fluids **24**, 2035 (1981).

[5]P. L. Colestock and R. J. Kashuba, Nucl. Fusion **23**, 763 (1983).

[6]D. G. Swanson, *Plasma Waves* (Academic, Boston, 1989), Chap. 6.

[7]K. Imre and H. Weitzner, Plasma Phys. Controlled Fusion (to be published).

[8]D. G. Swanson, Phys. Fluids **21**, 926 (1978).

[9]M. Bornatici, R. Cano, O. De Barbieri, and F. Engelmann, Nucl. Fusion **23**, 1153 (1983).